RevMexAA (Serie de Conferencias), **37**, 110–119 (2009)

SPECTROSCOPIC GRADIENTS IN EARLY-TYPE GALAXIES

A. Buzzoni,[1] C. Battistini,[2] L. Carrasco,[3] and E. Recillas[3]

RESUMEN

Discutimos aquí algunas propiedades relacionadas con la variación radial en los índices de Lick, Hβ, Mg_2 y FeI, para una muestra de 25 galaxias elípticas brillantes. Asimismo, analizamos la importancia de estos gradientes espectroscópicos como diagnósticos de los mecanismos físicos de formación galáctica. En este marco, proponemos tres escenarios evolutivos viables para explicar de forma consistente las características espectrales de las galaxias y por ello las propiedades evolutivas de sus poblaciones estelares.

ABSTRACT

We review some relevant properties of the observed changes of Hβ, Mg_2, and FeI Lick indices across the surface of 25 bright elliptical galaxies. The impact of these spectroscopic gradients is briefly discussed, in the framework of the leading physical mechanisms that led to galaxy formation. In particular, three relevant evolutionary scenarios are sketched, each one able, in principle, to consistently match galaxy spectral properties and effectively constrain the composing stellar populations in these systems.

Key Words: galaxies: elliptical and lenticular, cD — galaxies: evolution — galaxies: formation — galaxies: stellar content

1. INTRODUCTION

The discovery of intervening changes in the radial photometric properties of early-type galaxies has been one major achievement since early observing studies of this class of galaxies. Pioneering contributions by de Vaucouleurs (1961); Tifft (1963); Miller & Prendergast (1962, 1968) made clear, in fact, that ellipticals and S0 galaxies cannot be regarded as homogenous stellar systems; generally, their core appears "redder" (in terms of integrated broad-band colors) compared to a "bluer" outermost envelope.

This feature seems actually to characterize the entire galaxy population of the local Universe (including spirals) along the full range of mass and luminosity. However, while for spirals one can naturally invoke the ongoing star formation as the responsible mechanism for a bluer disk, the situation still remains much more unclear for ellipticals, widely recognized as old "quiescent" stellar systems.

A more explicit assessment of spectroscopic gradients within ellipticals, based on narrow-band photoelectric observations of the near-ultraviolet CN band at 4150 Å, has been first reported by McClure (1969), who remarked that *"the cyanogen absorption is found to be stronger in the central cores of the galaxies than in the surrounding areas of the nucleus"*, an evidence that led the author to conclude that *"stars in the central core of typical elliptical and spiral galaxies are super metal rich with respect to the majority of stars in the solar neighborhood"*.

The advent of the Lick narrow-band system (first defined by Faber et al. 1977, and further expanded and standardized by Worthey et al. 1994, and Trager et al. 1998), eased a more effective management of the spectroscopic output in order to quantify the radial trend of several absorption features in the optical wavelength range between 4000 and 6000 Å. This opened to a series of important contributions (Efstathiou & Gorgas 1985; Wirth 1985; Thomsen & Baum 1987; Peletier & Valentijn 1989; Gorgas et al. 1990; Carollo et al. 1993, just to mention only a few reference cases), which more systematically explored the problem of spectroscopic gradients within early-type galaxies.

A striking result that emerged from these studies is that "metals" may no longer be considered as a unitary family of elements, and they rather present large differences in the chemical partition among galaxies. In particular, there are distinct signs that Iron might be decoupled from Magnesium (and the rest of the so-called "α" elements) in the core of ellipticals (Worthey et al. 1992; Buzzoni et al. 1994; Lee & Worthey 2005), a fact that shed new light on the early chemical history of the galaxies and specifically on the selective role played by SNe.

[1]INAF-Osservatorio Astronomico di Bologna, Via Ranzani 1, 40127, Bologna, Italy (alberto.buzzoni@oabo.inaf.it).

[2]Dip. di Astronomia, Universitá di Bologna, Via Ranzani 1, 40127, Bologna, Italy.

[3]Instituto Nacional de Astrofísica, Óptica y Electrónica, Luis E. Erro 1, 72840 Tonantzintla, Puebla, Mexico.

On the other hand, theory readily suggested that a specific radial trend has to be expected for any metal feature, the amount and sign depending on the physical mechanisms that marked galaxy genesis. In particular, the imposing theoretical scenario of "hierarchical" galaxy formation (White & Frenk 1991; Kauffmann et al. 1994; Navarro et al. 1997) predicted bright galaxies to grow "from inside out" through a "coalescence" of primeval metal-poor stellar systems of lower mass. Conversely, in the alternative "monolithic" scenario (Larson 1975, 1974), ellipticals basically proceeded from the gravitational collapse of primeval gas clouds that led to a chemically enhanced galaxy core, richer in metals compared to the external regions.

Facing the different theoretical scenarios, it is clear, therefore, that the study of galaxy spectroscopic gradients can give in principle valuable clues on the way these bright systems eventually formed. In this framework, we would like to contribute to the current debate by briefly reporting here on a long-term programme carried out by our group at the Mexican telecopes along the last decade, aimed at detecting and studying spectral gradients within a large sample of bright ellipticals mainly belonging to the Virgo Cluster and the Leo Group, but also exploring looser "field" environment conditions. This contribution partly follows up early preliminary results (Buzzoni 1995a; Carrasco et al. 1995) and summarizes some of the relevant results more exhaustively discussed in a forthcoming paper (Buzzoni et al., in preparation).

2. THE OBSERVING DATABASE

Our observations have entirely been collected at the two 2.12 m Mexican telescopes of the National Observatory at San Pedro Mártir (hereafter referred to as SPM) and at the Cananea Guillermo Haro National Astrophysics Observatory (CNN) along several observing runs between years 1992 and 1997. Both telescopes were equipped with a long-slit Böller & Chivens Cassegrain spectrograph. We worked at mid-resolution, using a 600 gr/mm grating for SPM observations and a 300 gr/mm grating for CNN data. These provided an inverse dispersion of 86 Å/mm (SPM) and 67 Å/mm (CNN) along a 4200–6000 Å wavelength interval. Slit width was tuned up such as to provide a quite similar spectral resolution between 5 and 6 Å (FWHM) throughout.

The SPM observing campaign gathered data for 18 elliptical and S0 galaxies, while a supplementary list of 24 targets was observed at CNN. Once considering a large overlapping fraction (16 objects in common) between the SPM and CNN runs, this eventually led to a whole sample of 25 galaxies. The large overlap between SPM and CNN observations allowed us to secure an accurate assessment of sky contamination on the galaxy spectra, a critical effect that has been independently sized up via two different observing strategies.

TABLE 1

THE SPM AND CNN GALAXY DATABASE

Name	SPM	CNN	Name	SPM	CNN
NGC 0194	yes	yes	NGC 4278	yes	yes
NGC 0524	yes	yes	NGC 4365	no	yes
NGC 1201	yes	yes	NGC 4374	yes	yes
NGC 1395	yes	yes	NGC 4382	yes	yes
NGC 1587	yes	yes	NGC 4472	yes	yes
NGC 2549	yes	yes	NGC 4742	yes	no
NGC 2685	yes	yes	NGC 4649	yes	yes
NGC 2764	no	yes	NGC 5576	no	yes
NGC 3245	yes	yes	NGC 5846	no	yes
NGC 3489	yes	yes	NGC 5866	no	yes
NGC 3607	yes	yes	NGC 5982	no	yes
NGC 4111	yes	yes	NGC 6166	no	yes
NGC 4125	yes	yes			

In order to confidently reach the most vanishing external regions of the galaxies (typically at $S/N \gtrsim 100$ per wavelength resolution element), our spectroscopy required very deep exposures (up to 3.5 hr integration time). In the most favourable cases this allowed us to probe galaxy spectral energy distribution (SED) up to 6 effective radii (r_e), although our analysis had usually to restrain to the inner r_e region, depending on galaxy apparent size compared to the CCD field of view. Table 1 gives a summary of the galaxy sample collected during the SPM and CNN observing runs.

As described in more detail in Buzzoni et al. (2009), the reduction procedure was carried out with the ESO package MIDAS adopting the standard routines of the LONGSLIT context. Each set of original frames was properly bias subtracted while the CCD high-frequency noise was recovered by dividing by a normalized mean flat-field taken each night with a halogen lamp inside the spectrograph. Spectra of a He/Ar lamp, taken frequently during each night provided the wavelength calibration, and comparison with several standard stars provided the appropriate flux conversion of CCD output

2.1. *A major caveat: the sky subtraction*

Special care has been devoted, throughout the observing runs, to a proper sampling of sky emission close to each target galaxy. This measure is in fact mandatory to accurately trace galaxy luminosity at large radii, where target surface brightness drops to nominal values compared to the surrounding diffuse background. In addition to the few telluric emission lines, in the wavelength range of our observations sky spectral continuum basically originates from the solar light scattered by the upper layers of Earth atmosphere. When neglected, or not properly subtracted, this spurious contribution can strongly affect the inferred galaxy SED in the faintest external regions making absorption features to display a fake "solar look".

In order to optimize this delicate task, we tried two different observing strategies. Taking advantage of a wider field of view of SPM frames, we centered the galaxy on the spectrograph slit such as to reach the sky level at least at one of the CCD edges. The obvious advantage of a parallel galaxy and sky sampling within the same frame was, however, largely limited by the intervening vignetting effects across the longslit, that eventually added further uncertainty to an accurate sky subtraction.

A more prudent but much more time consuming strategy was devised, on the contrary, for CNN observations, where a smaller CCD coverage required to interpolate sky emission by taking two separate frames, before and after each scientific observation, and with the same exposure time. The drawback, in the latter case, is that the procedure does not necessarily account in a better way for any abrupt change in the atmospheric conditions along the galaxy scientific exposure.

In both cases, therefore, we had to further "tune up" the amount of sky level to be eventually subtracted to galaxy intensity profile along the spatial coordinate of the spectrograph longslit, such as to recover the corresponding effective radius, as reported in the literature (for instance, in the RC3 Catalog, de Vaucouleurs et al. 1995).[4] In this regard, one has to recall that, by definition, half the galaxy total luminosity is encircled within one effective radius,

$$r_e = \sqrt{r_a \times r_b} = r_a \sqrt{1-\epsilon}\,, \tag{1}$$

being the galaxy major and minor semi-axes, r_a and r_b respectively, related to the apparent eccentricity $\epsilon = 1 - r_b/r_a$. As our longslit was typically aligned along the galaxy major axis, the previous constraint

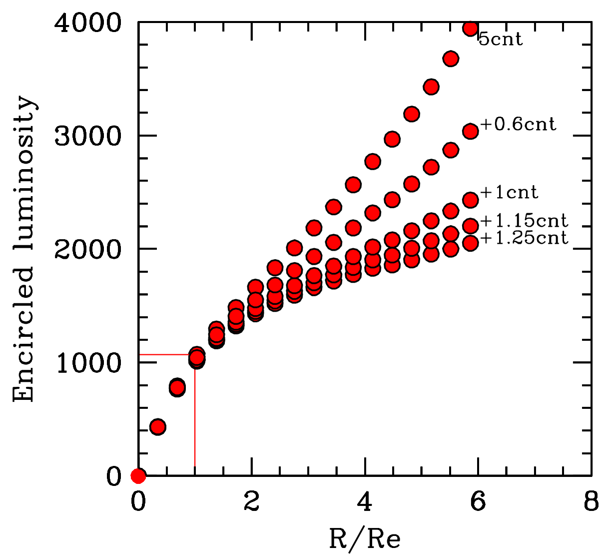

Fig. 1. An illustrative example of "tuned" sky subtraction for the case of galaxy NGC 3489. The galaxy encircled luminosity (expressed in ADU units) has been computed, according to the observed spatial profile along the spectrograph longslit. The nominal value of the sky luminosity to be subtracted (originally set by the observations at about 5 ADU counts in this specific case, as labelled on the upper curve) has been further increased in the other curve shelf such as to make roughly a half of the residual (asymptotic) luminosity of the galaxy to be encircled within one effective radius (R_e). For this case, an optimum solution is achieved by further increasing the nominal sky level by $\sim 25\%$ to ~ 6.2 ADU counts.

implies that

$$\int_0^{r(a)} [I_{\rm obs}(x) - {\rm Sky}]\, x\, dx \simeq \int_{r(a)}^{\infty} [I_{\rm obs}(x) - {\rm Sky}]\, x\, dx, \tag{2}$$

where $I_{\rm obs} = (I_{\rm gal} + {\rm Sky})$ is the raw galaxy intensity and x is the spatial coordinate along the slit, centered on the galaxy photometric peak in the frame. Clearly, the sky contamination especially affects the r.h. side of equation (2) (as $I_{\rm gal} \ll$ Sky), and its level can therefore be accurately set such as to balance the two sides of the equation. In some cases, our correction procedure led to a small offset in the CCD background counts, of the order of ± 1 ADU. This is equivalent to a $\sim 25\%$ relative uncertainty in the sky level, as shown in the illustrative experiment of Figure 1, for the case of NGC 3489.

2.2. *Lick indices and their diagnostic properties*

As well known, a straightforward way to summarize galaxy spectrophotometric properties is to

[4] Note that by overestimating sky level we artificially "sharpen" galaxy surface brightness profile inducing a smaller effective radius. On the other hand, by underestimating sky emission, we leave further spurious luminosity to galaxy external regions, thus mimicking a larger value of r_e.

rely on narrow-band indices, measuring the apparent strength of the main absorption features in the integrated SED. As far as the optical wavelength is concerned, the Lick index system is by far the most popular and extensively used one as it covers practically every relevant feature that marks the spectrum of stars and stellar systems between 4100 and 6200 Å. Operationally, each index in the system derives from a measure of the feature strength (f_f, computed by averaging the observed flux through a wavelength window of width Δ_f, centered on the relevant absorption line) relative to the adjacent pseudocontinuum level (f_c) probed at two side windows. Once the ratio f_c/f_f is computed, the index easily derives in terms of pseudoequivalent width of the absorption feature, namely

$$I_{\rm EW} = \Delta_f \left(1 - \frac{f_f}{f_c}\right) , \qquad (3)$$

or, in magnitude unit:

$$I_{\rm mag} = -2.5\ \log\left(\frac{f_f}{f_c}\right) . \qquad (4)$$

Both formalisms are physically equivalent, as

$$I_{\rm EW} = \Delta_f \left(1 - 10^{-0.4\, I_{\rm mag}}\right) , \qquad (5)$$

although the magnitude notation better applies to molecular indices, while pseudoequivalent width notation is usually preferred for atomic line indices (Worthey et al. 1994).

Facing a quite simple operational definition, however, a correct interpretation of index output requires some important cautions as

(i) the index calibration scale is a fully empirical one, and always requires the observation of a convenient grid of primary or secondary standard stars;

(ii) spectra must reproduce a standard spectral resolution of 7–8 Å (FWHM). While observations taken at higher resolution can easily be degraded, the opposite cannot straightforwardly be carried out.

(iii) to a more detailed analysis, most indices comprise in fact blended features of several lines, with a composite contribution of three or four different elements (in great majority FeI, mixed with other neutral metals).

(iv) the index set is not completely "independent" as in some cases different index bands fully or partially overlap, then sampling the same wavelength interval and providing therefore a physically redundant piece of information. An outstanding case, in this regard, is that of the FeI index at 5335 Å, fully comprised into the red continuum band of the molecular Mg_2 index (see Figure 2).

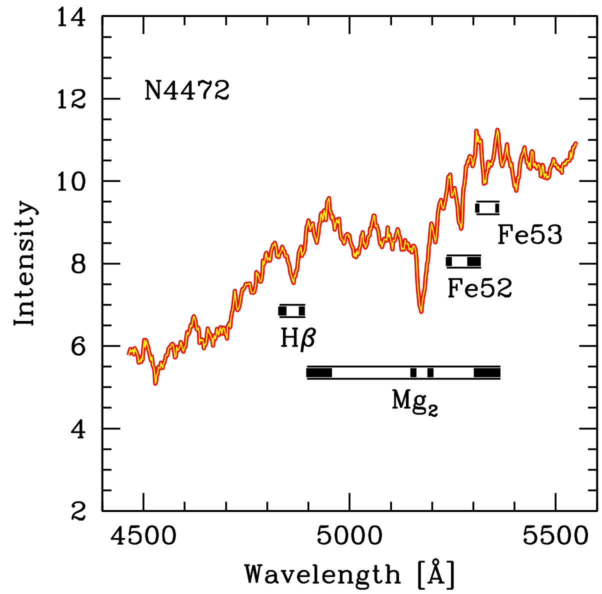

Fig. 2. A sketch of the Lick index definition superposed to the spectrum of galaxy NGC 4472. The feature windows and the two side bands probing the pseudocontinuum level are marked as tick lines for the Hβ, Mg_2, Fe5270 and Fe5335 indices, according to Worthey's et al. (1994) definition.

Within the full range of Lick indices covered by our spectral observations, we want to briefly discuss, in this report, the results dealing with the popular sub-set that comprises the Hβ, Mg_2, Fe5270 and Fe5335 features. Both the Balmer line and the striking MgH molecular feature in fact characterize the spectra of elliptical galaxies in the visual range and have been the subject of extensive investigation in previous studies (see, among others, Worthey & Ottaviani 1997; Tantalo et al. 1998; Vazdekis & Arimoto 1999; Maraston & Thomas 2000; Tantalo & Chiosi 2004a; Thomas et al. 2004). In addition, although much less prominent and with some marginal contamination by CaI, the two FeI lines at 5270 and 5335 Å are also useful tracers of metal abundance.

Following a theoretical approach based on population synthesis models, Buzzoni (1995b) first showed that this specific sub-set of narrow-band indices actually provides an optimum tool to probe the main morphological features of the (unresolved) C-M diagram of composing stars in distant ellipticals. From one hand, in fact, the Hβ line is found to effectively trace the warmest stellar component in a system, and it reaches its maximum strength in stars about $T_{\rm eff} \simeq 8,000 - 10,000$ K (Buzzoni et al. 1994). In the integrated SED of any old and intermediate-

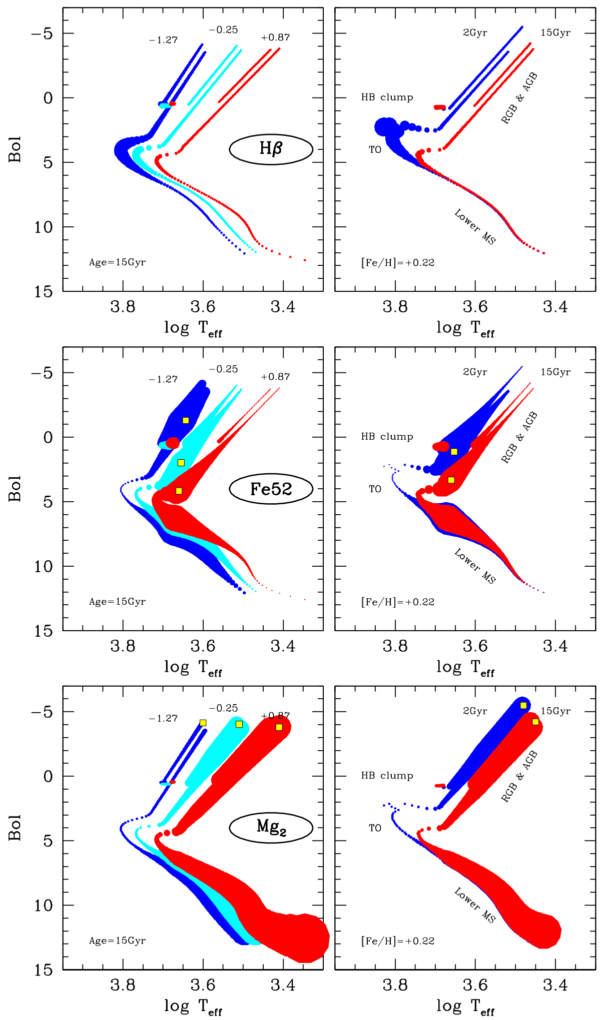

Fig. 3. Theoretical H-R diagrams for a set of SSPs from the Buzzoni (1989, 1995b) synthesis code. Line thickness traces the strength of Hβ (top panel), Fe5270 (middle panel) and Mg_2 (bottom panel) Lick indices for stars along the different evolutionary branches in each diagram. SSPs of either different metallicity (left panels) or age (right panels) are considered, as labelled on the plots. Note that while Hβ and Mg_2 peak respectively at the warmest and coolest temperature edges of stellar distribution, the maximum Fe5270 (and similarly Fe5335) index marks the core of the H-R temperature distribution, for stars about $T_{\rm eff} \simeq 4500$ K.

age stellar population this index is therefore especially sensitive to the temperature location of the Main Sequence Turn Off (MSTO) region.

On the other hand, by responding to the MgH molecular strength, the Mg_2 index is a fair tracer of the coolest red giant stars and its integrated strength gives a hint of their relative contribution at optical wavelengths (Buzzoni et al. 1992). This is clearly shown in Figure 3 for an illustrative collection of simple stellar population (SSP) models from the Buzzoni (1989, 1995b) synthesis code. As far as the integrated SED of a stellar aggregate is concerned, note from the figure that Hβ and Mg_2 indices are in fact essential to effectively constrain the blue and red *color edges* of the unresolved C-M diagram of the composing stars.

In addition, the Fe indices add a further important piece of information to our analysis, as their strongest stellar contributors trace the "core" of the C-M temperature distribution, probing stars around the base of the red giant branch (see, again, Figure 3).

3. SPECTROSCOPIC GRADIENTS

The resulting radial trend for the considered subset of Lick indices is summarized in the series of Figures 4 and 5. For the illustrative scope of this contribution we just displayed the case of four well recognized early-type galaxies, namely NGC 3489 (type S0), 4111 (S0), 4125 (E6) and 4472 (E2).

The plots provide a vivid example of the inherent difficulty in tracing SED properties at large distances from galaxy center. This is a natural consequence of the very sharp surface-brightness profile of ellipticals, where the observation of the outermost regions quickly becomes noise-limited. For this reason, moving outward from galaxy centre we had to average the spatial information by rebinning the spectrum with increasing width such as to preserve (as far as possible) measurement accuracy[5].

Figures 4 and 5 are clearly suggestive of some leading properties of our spectroscopic sample:

(i) as a general pattern, both Iron lines and α elements (as traced by the Mg_2 index) move accordingly, and become shallower when increasing galaxy radius;

(ii) conversely, Hβ index mostly tends to bunch around a constant value, which basically indicates a lack of any systematic radial gradient. If any, as for the case of NGC 4111 reported here, a positive correlation seems to be in place with the Mg_2 and Fe indices, as summarized in Figure 6. Overall, our sample indicates $\Delta H\beta/\Delta \log r = -0.23 \pm 0.33$ (Carrasco et al. 1995).

Further useful pieces of information can also be added, by accounting for previous preliminary dis-

[5] Compared to the observation of galaxy core region, say within the inner $0.2\,r_e$ radius, and assuming a standard de Vaucouleurs brightness profile as a reference, one has to roughly increase spatial binning by a factor of two at $1\,r_e$, or a factor of three at $2\,r_e$ to maintain a roughly constant S/N in the co-added spectrum.

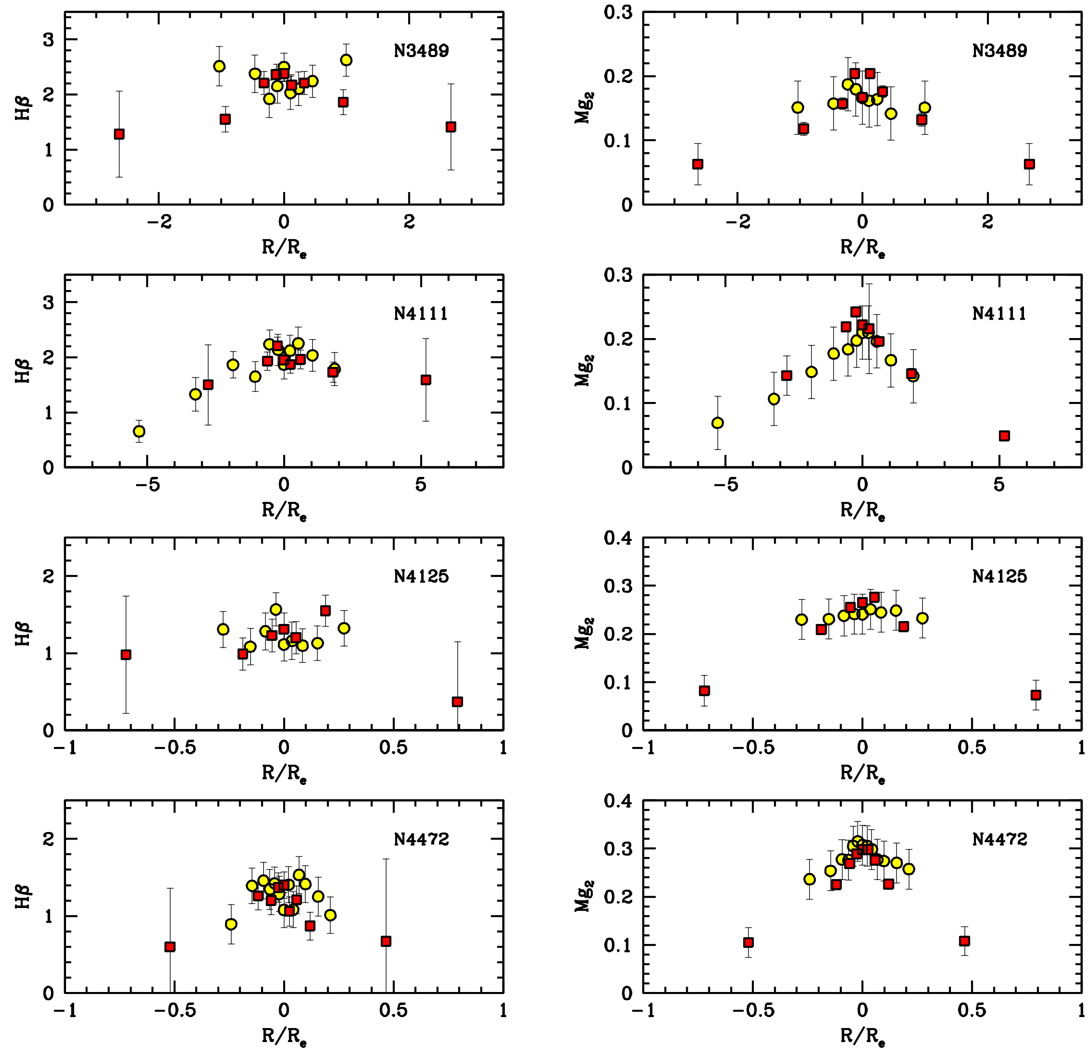

Fig. 4. Observed radial changes of the Hβ and Mg_2 indices for the illustrative cases of galaxies NGC 3489, 4111, 4125 and 4472 in our sample. Both SPM (square markers) and CNN (dot markers) are reported. All the data have been converted to the Lick standard system. In all cases, spectrograph longslit was probing galaxy major axis. Radial distance from the center is reported in unit of galaxy effective radius R_e.

cussions of our galaxy sample, as in Buzzoni (1995a) and Carrasco et al. (1995). In particular,

(iii) although with a large individual scatter, nebular contribution to galaxy SED, as traced by the [OIII] 5007 Å emission, is on average stronger among low-mass ellipticals and strongly core-concentrated Buzzoni (1995a); this is partly in consequence of a larger fraction of residual gas within dwarf galaxies and of their younger (bluer) stellar population;

(iv) a debated (and yet unsettled) question concerns the possible impact of triggering mechanisms that cause [OIII] nebular emission on the Balmer-line emission as well. A positive correlation was originally found by Gonzalez (1992) between equivalent widths of the two emission lines, in the form of $\Delta H\beta = 0.7$[OIII], but this result does not seem to be supported by our data, as already shown by Carrasco et al. (1995).

4. INDEX TREND AMONG AND WITHIN ELLIPTICAL GALAXIES

As a further step in our analysis, it could be of special interest to assess the problem of galaxy spectroscopic gradients in a more general framework, contrasting the observed relationship of spectral features, as seen *within* each individual galaxy of our sample with the overall index distribution *among* galaxies as traced by their core measurements. In this regard, several outstanding contributions in the

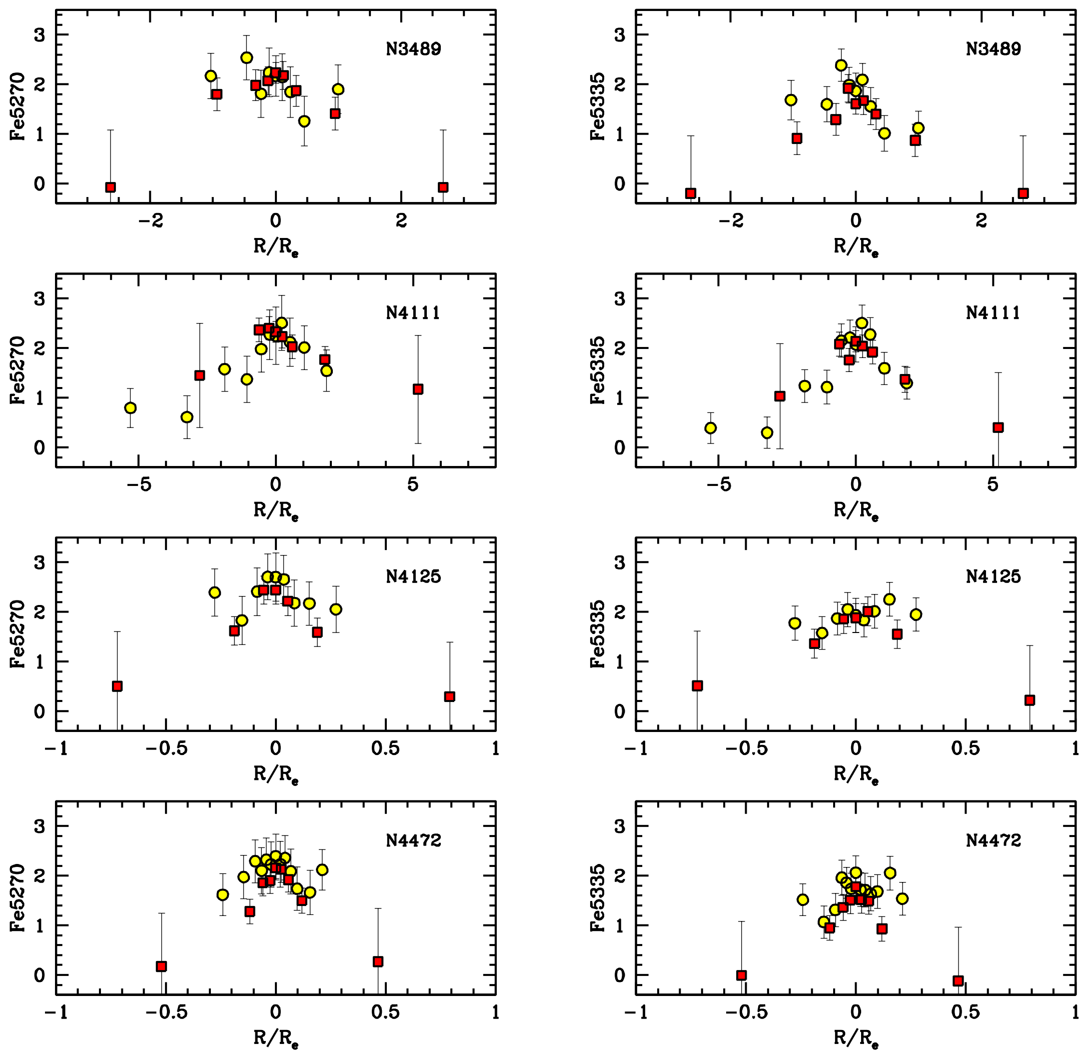

Fig. 5. As for Figure 4, but for the FeI Lick indices, Fe5270 and Fe5335.

past decades have set the reference interpretative framework. We should recall the "7-Samurai" work (Davies et al. 1987; Burstein et al. 1987) or the contribution by Sandra Faber and collaborators (Faber & Jackson 1976; Worthey et al. 1992; Bender et al. 1992), just to mention only a few milestones.

Our results can be summarized by the two panels of Figure 7. In the figure, triangles mark the core values of the Lick indices for each galaxy in our sample, while the radial run of the indices is sketched by the vectors connecting with the observed (or linearly extrapolated) values at r_e (solid dots in each panel). In both plots, therefore, the index distribution *among* ellipticals is traced by the small triangles, while the index correlation *within* galaxies is traced by the sketched vectors.

4.1. *The puzzling case of Hβ*

Just a glance to the figure makes clear that the observed trends *among* and *within* galaxies are different. By itself, this striking evidence points to a substantially different nature of physical mechanisms that led stellar populations to differentiate inside and among galaxies.

As a first relevant feature, in this regard, note in the left panel of Figure 7 that the triangle distribution indicates that low-Mg_2 ellipticals also display a stronger Hβ index, thus confirming a well recognized *negative* correlation between Balmer absorption lines and Magnesium (Worthey & Ottaviani 1997; Tantalo & Chiosi 2004b; Vazdekis et al. 2004). Conversely, and quite remarkably, *this trend is not reproduced along galaxy radius*, and Hβ shows there a roughly steady or a mildly *positive* correlation with Mg_2.

To add further to our trouble, the situation seems to reverse as far as the Fe vs. Mg distribution is concerned (see right panel of Figure 7). In the latter case, in fact, data show an apparent constant Fe5270 index distribution *among* galaxies with varying core Mg_2 values (Buzzoni et al. 1994; Worthey et al. 1992); on the contrary, a nice positive correlation is in place *within* galaxies, with all the metal lines becoming shallower when moving at larger distances from the galaxy center.

5. RADIAL GRADIENTS AND IMPLIED EVOLUTIONARY SCENARIOS

If metallicity is the main running parameter along galaxy radius (as the Fe5270 vs. Mg_2 correlation might lead to conclude), then we should expect bluer (metal-poorer) stellar populations to prevail as far as we move to larger distances from galaxy center. This argument would easily give reason of the observed color gradients (i.e. a "redder" core typically surrounded by a "bluer" outer envelope). On the other hand, as a natural consequence, this trend would also lead to an increasingly warmer MSTO point in the C-M diagram of external stellar populations compared to the core situation (see Figure 3), and this directly calls for a *negative* correlation between Balmer and metal lines, contrary to what we observe.

To reconcile this apparent dichotomy we can invoke at least three different "variants" to the standard evolutionary scenario, each one potentially able to recover the puzzling behaviour of Hβ.

(1) *Age changes* may play a role, as a further intervening parameter in modulating galaxy spectrophotometric properties, in consequence of the physical mechanisms that led to galaxy formation. In particular, in case of a monolithic scenario, we expect "chemical cooking" to have further proceeded and in shorter dynamical timescale among high-mass systems. Besides being metal rich, these galaxies are therefore also older (i.e. "redder") than low-mass systems. For the latter, on the contrary, a longer dynamical timescale led to a slower chemical enhancement and left room for a silent residual star formation after the primeval starburst. This argument would naturally account for the negative Hβ vs. Mg_2 correlation of the integrated indices of Figure 7, and it would also agree with the observed color-magnitude relation seen among cluster ellipticals Visvanathan & Sandage (1977). In addition, it would also consistently explain why the observed [OIII] nebular emission is usually more enhanced among dwarf ellipticals (see Figure 3 in Buzzoni 1995a).

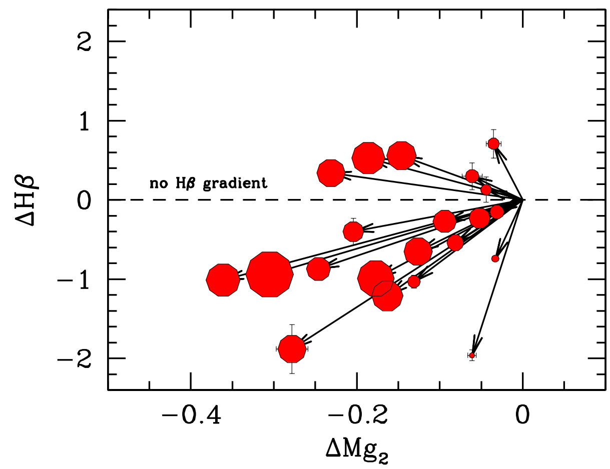

Fig. 6. Observed changes of Hβ and Mg_2 indices along one galaxy effective radius. The core index value is taken as a zero point for each galaxy. The big dot is proportional to galaxy mass, through the measured value of the spectral velocity dispersion, σ_v. Note the lack of any systematic correlation between the two indices.

Nevertheless, any age gradient might barely account for the observed trend of the Lick indices *within* the individual galaxy. In fact, a flat Hβ radial trend would generally imply a younger metal-rich core, especially for bright (high-mass) ellipticals, and this is clearly at odds with the observed small value of integrated Hβ index (Buzzoni et al. 1994; Worthey & Ottaviani 1997).

(2) *The "α-elements decoupling* could be a second possibility to explain the observed radial trends of galaxy spectrophotometric indices. Models predict in fact that by selectively enhancing the relative contribution to Z by metals produced via α-particle accretion in nuclear reactions (i.e. C, O, Mg, Si, Ca, Ti etc.) typically reflects on stellar tracks in a slightly cooler (redder) MSTO point. This in consequence of the enhanced efficiency of CNO nuclear reactions that allows a lower surface temperature for MS stars (Bergbusch & Vandenberg 1992; Salaris et al. 1993).

As a result, some intervening enhancement of α-element contribution among stellar populations at large galactic radii might, in principle, compensate for the MSTO blueing due to the low-metallicity regime, thus assuring a roughly constant value of Hβ while leaving unchanged the eventual correlation between Iron and Magnesium indices. To further reinforce our speculation, note that this scenario has actually been confirmed since long by the direct observation of α-enhanced stars among metal-poor stel-

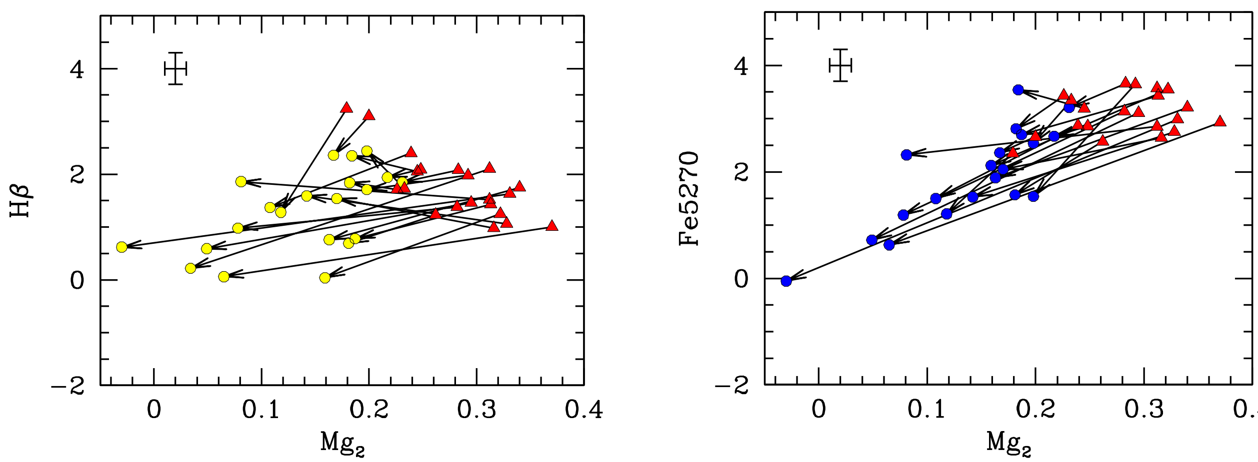

Fig. 7. Derived trend of the Lick indices along galaxy radius for the observed sample of ellipticals. For each galaxy, arrows connect the index values at the core region (triangles) with the measurements at one effective radius (dots). Note, for both index combinations in the panels, the different trend of Hβ vs. Mg$_2$, and Fe5270 vs. Mg$_2$ *among* the elliptical galaxy population and *within* each system. See text for a full discussion of this important point.

lar populations of Galactic globular clusters and in the Galaxy disk (see, e.g. Gratton et al. 1996).

If this the case, then the apparent decoupling between "α" elements and Fe metal group in ellipticals would further cconstrain the selective metal enrichment of early-type galaxies via Supernovae of the different types.

(3) *A blue horizontal-branch (HB) morphology* for metal-rich stellar populations in the galaxy core is our third possibility to self-consistently recover the observed spectrophotometric gradients of ellipticals. The issue directly relates with the so-called "second-parameter dilemma", extensively studied in the Galactic globular cluster environment, aimed at detecting the distinctive parameter (in addition to cluster metallicity) able to break in some cases the monotonic relationship between HB morphology and [Fe/H]. The "standard" scenario forsees in fact an increasingly redder and "clumped" HB stellar distribution for populations with increasing [Fe/H] (Renzini 1983); this, in consequence of a higher He core mass supplied at the end of the red-giant evolution (Sweigart & Gross 1976; Dorman 1992; Piersanti et al. 2004; Serenelli & Weiss 2005).

On this line, an important variant to the standard picture may occur once considering metal-rich stellar populations beyond the range of globular clusters, as in the core of bright elliptical galaxies, indeed. Possibly eased by a stronger mass loss via stellar wind, for solar or super-solar metal abundance theoretical models predict HB morphology to "bounce back" to a broader temperature distribution, with stars as hot as 30,000 K or more populating the ultraviolet region of the stellar C-M diagram (D'Cruz et al. 1996; Buzzoni & González-Lópezlira 2008).

When conveniently tuned up, the presence of such a hot stellar component in the core of old high-mass ellipticals might help explain the steady trend of Hβ still maintaining the observed Mg-Fe index correlation. Among others, a further major point of this scenario is that it may consistently account also for the striking "UV-upturn" phenomenon (Code & Welch 1979; Burstein et al. 1988), that is with the raising ultraviolet emission shortward of 2500 Å that seems to characterize the core properties of high-mass ellipticals (O'Connell 1999).

At the present stage of our knowledge, and facing the relevant *pros and cons* in consistently accounting for spectral properties of elliptical galaxies over the entire range of distinctive features, it is difficult to set any decisive argument in favor of one of these three envisaged scenarios. Overall, age spread (i.e. case 1 of previous discussion) might more likely play a central role differentiating integrated spectrophotometric properties among early-type galaxy systems of different mass. On the contrary, α-enhancement processes (case 2) and HB "bounced-back" morphology (case 3) might concur (and perhaps coexist) to mark the distinctive spectral feature across galaxy surface. If this is the case, then a careful study of the UV-upturn phenomenon and a further extension of galaxy spectroscopic studies at higher spectral resolution could, in the near future, hopefully shed light on the intimate mechanisms at work in elliptical galaxy evolution.

We acknowledge with pleasure the INAOE for partial financial support. One of us (A.B.) would like to thank the Organizers of this conference for the kind invitation and for such a friendly and enjoyable tribute to Luis Carrasco's work.

REFERENCES

Bender, R., Burstein, D., & Faber, S. M. 1992, ApJ, 399, 462
Bergbusch, P. A., & Vandenberg, D. A. 1992, ApJS, 81, 163
Burstein, D., Bertola, F., Buson, L. M., Faber, S. M., & Lauer, T. R. 1988, ApJ, 328, 440
Burstein, D., Davies, R. L., Dressler, A., Faber, S. M., Stone, R. P. S., Lynden-Bell, D., Terlevich, R. J., & Wegner, G. 1987, ApJS, 64, 601
Buzzoni, A. 1989, ApJS, 71, 817
———. 1995a, ASP Conference Ser. 86, Fresh Views of Elliptical Galaxies, ed. A. Buzzoni, A. Renzini, & A. Serrano (San Francisco:ASP), 189
———. 1995b, ApJS, 98, 69
Buzzoni, A., Gariboldi, G., & Mantegazza, L. 1992, AJ, 103, 1814
Buzzoni, A., & González-Lópezlira, R. A. 2008, ApJ, 686, 1007
Buzzoni, A., Mantegazza, L., & Gariboldi, G. 1994, AJ, 107, 513
Carollo, C. M., Danziger, I. J., & Buson, L. 1993, MNRAS, 265, 553
Carrasco, L., Buzzoni, A., Salsa, M., & Recillas-Cruz, E. 1995, ASP Conference Ser. 86, Fresh Views of Elliptical Galaxies, ed. A. Buzzoni, A. Renzini, & A. Serrano (San Francisco:ASP), 235
Code, A. D., & Welch, G. A. 1979, ApJ, 228, 95
Davies, R. L., Burstein, D., Dressler, A., Faber, S. M., Lynden-Bell, D., Terlevich, R. J., & Wegner, G. 1987, ApJS, 64, 581
D'Cruz, N. L., Dorman, B., Rood, R. T., & O'Connell, R. W. 1996, ApJ, 466, 359
de Vaucouleurs, G. 1961, ApJS, 5, 233
de Vaucouleurs, G., de Vaucouleurs, A., Corwin, H. G., Buta, R. J., Paturel, G., & Fouque, P. 1995, VizieR Online Data Catalog, 7155, 0
Dorman, B. 1992, ApJS, 80, 701
Efstathiou, G., & Gorgas, J. 1985, MNRAS, 215, 37P
Faber, S. M., & Jackson, R. E. 1976, ApJ, 204, 668
Faber, S. M., Burstein, D., & Dressler, A. 1977, AJ, 82, 941
Gonzalez, J. J. 1992, PhD Thesis, Univ. of California, Santa Cruz, USA
Gorgas, J., Efstathiou, G., & Aragon Salamanca, A. 1990, MNRAS, 245, 217
Gratton, R., Carretta, E., Matteucci, F., & Sneden, C. 1996, ASP Conference Ser. 92, Formation of the Galactic Halo...Inside and Out, ed. H. Morrison & A. Sarajedini (San Francisco: ASP), 307
Kauffmann, G., Guiderdoni, B., & White, S. D. M. 1994, MNRAS, 267, 981
Larson, R. B. 1974, MNRAS, 166, 585
———. 1975, MNRAS, 173, 671
Lee, H.-c., & Worthey, G. 2005, ApJS, 160, 176
Maraston, C., & Thomas, D. 2000, ApJ, 541, 126
McClure, R. D. 1969, AJ, 74, 50
Miller, R. H., & Prendergast, K. H. 1962, ApJ, 136, 713
———. 1968, ApJ, 153, 35
Navarro, J. F., Frenk, C. S., & White, S. D. M. 1997, ApJ, 490, 493
O'Connell, R. W. 1999, ARA&A, 37, 603
Peletier, R. F., & Valentijn, E. A. 1989, Ap&SS, 156, 127
Piersanti, L., Tornambé, A., & Castellani, V. 2004, MNRAS, 353, 243
Renzini, A. 1983, Mem.S.A.It, 54, 335
Salaris, M., Chieffi, A., & Straniero, O. 1993, ApJ, 414, 580
Serenelli, A., & Weiss, A. 2005, A&A, 442, 1041
Sweigart, A. V., & Gross, P. G. 1976, ApJS, 32, 367
Tantalo, R., & Chiosi, C. 2004a, MNRAS, 353, 405
———. 2004b, MNRAS, 353, 917
Tantalo, R., Chiosi, C., & Bressan, A. 1998, A&A, 333, 419
Thomas, D., Maraston, C., & Korn, A. 2004, MNRAS, 351, L19
Thomsen, B., & Baum, W. A. 1987, ApJ, 315, 460
Tifft, W. G. 1963, AJ, 68, 302
Trager, S. C., Worthey, G., Faber, S. M., Burstein, D., & Gonzalez, J. J. 1998, ApJS, 116, 1
Vazdekis, A., & Arimoto, N. 1999, ApJ, 525, 144
Vazdekis, A., Trujillo, I., & Yamada, Y. 2004, ApJ, 601, L33
Visvanathan, N., & Sandage, A. 1977, ApJ, 216, 214
White, S. D. M., & Frenk, C. S. 1991, ApJ, 379, 52
Wirth, A. 1985, ApJ, 288, 132
Worthey, G., Faber, S. M., & Gonzalez, J. J. 1992, ApJ, 398, 69
Worthey, G., Faber, S. M., Gonzalez, J. J., & Burstein, D. 1994, ApJS, 94, 687
Worthey, G., & Ottaviani, D. L. 1997, ApJS, 111, 377